

This is a self-archived version of an original article. This version may differ from the original in pagination and typographic details.

Author(s): Kinnunen, Sami; Arstila, Kai; Sajavaara, Timo

Title: Al₂O₃ ALD films grown using TMA + rare isotope ²H₂¹⁶O and ¹H₂¹⁸O precursors

Year: 2021

Version: Accepted version (Final draft)

Copyright: © 2020 Elsevier

Rights: CC BY-NC-ND 4.0

Rights url: <https://creativecommons.org/licenses/by-nc-nd/4.0/>

Please cite the original version:

Kinnunen, S., Arstila, K., & Sajavaara, T. (2021). Al₂O₃ ALD films grown using TMA + rare isotope ²H₂¹⁶O and ¹H₂¹⁸O precursors. *Applied Surface Science*, 546, Article 148909.
<https://doi.org/10.1016/j.apsusc.2020.148909>

Journal Pre-proofs

Full Length Article

Al₂O₃ ALD films grown using TMA + rare isotope ²H₂¹⁶O and ¹H₂¹⁸O precursors

S. Kinnunen, K. Arstila, T. Sajavaara

PII: S0169-4332(20)33668-0

DOI: <https://doi.org/10.1016/j.apsusc.2020.148909>

Reference: APSUSC 148909

To appear in: *Applied Surface Science*

Received Date: 17 August 2020

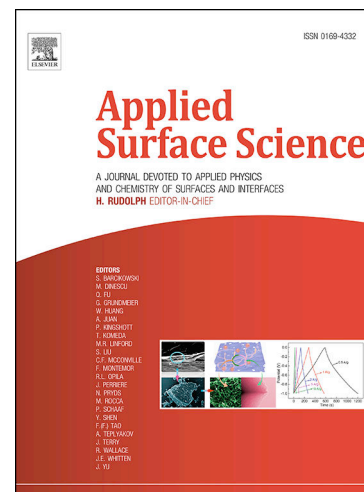
Revised Date: 17 December 2020

Accepted Date: 30 December 2020

Please cite this article as: S. Kinnunen, K. Arstila, T. Sajavaara, Al₂O₃ ALD films grown using TMA + rare isotope ²H₂¹⁶O and ¹H₂¹⁸O precursors, *Applied Surface Science* (2020), doi: <https://doi.org/10.1016/j.apsusc.2020.148909>

This is a PDF file of an article that has undergone enhancements after acceptance, such as the addition of a cover page and metadata, and formatting for readability, but it is not yet the definitive version of record. This version will undergo additional copyediting, typesetting and review before it is published in its final form, but we are providing this version to give early visibility of the article. Please note that, during the production process, errors may be discovered which could affect the content, and all legal disclaimers that apply to the journal pertain.

© 2020 Published by Elsevier B.V.



Al₂O₃ ALD films grown using TMA + rare isotope ²H₂¹⁶O and ¹H₂¹⁸O precursors

S. Kinnunen¹, K. Arstila¹ and T. Sajavaara¹

¹University of Jyväskylä, Department of Physics, P. O. Box 35, FI-40014 University of Jyväskylä, Finland

Abstract

In this work hydrogen and oxygen migration and exchange reactions in the atomic layer deposited (ALD) Al₂O₃ thin films were studied together with hydrogen incorporation by varying deposition parameters. Al₂O₃ films deposited at low temperatures can contain more than 20 at. % of hydrogen. Both higher temperature and longer purge length decrease the hydrogen and carbon concentrations significantly. In order to track the hydrogen and oxygen movement in the films, heavy water (²H₂¹⁶O) and oxygen-18 enriched water (¹H₂¹⁸O) were used as precursors in combination with trimethylaluminium (TMA). Different isotopes of the same element were quantified by means of time-of-flight elastic recoil detection analysis (ToF-ERDA). It was found out that ¹H/²H exchange reactions take place even at room temperature if the hydrogen concentration is high enough. On the other hand, oxygen atoms in the films do not migrate notably.

Keywords: ALD, Al₂O₃, Low temperature, Heavy water, Hydrogen migration, TMA

1. Introduction

Atomic layer deposited (ALD) amorphous aluminium oxide (Al_2O_3) is both extensively used and much studied thin film material. Alumina films have been studied, for example, as a high-k material for semiconductor industry [1–3] as well for gas permeation barriers [4–6]. There are numerous ALD processes for Al_2O_3 but especially the process with trimethylaluminium (TMA) and water as precursors is widely studied (www.atomiclimits.com ALD database mentions almost 300 articles as to date [7]) and the reaction mechanism is also believed to be quite well understood [8, 9].

One early identified application for amorphous ALD-oxide films has been to use it for moisture and gas permeation barriers [10]. Thin moisture barriers are needed in packaging materials where flexibility of the barrier is of importance. Another example is organic light emitting diodes (OLED) which require transparent moisture barrier. OLEDs are known to be sensitive to water vapour and oxygen, and in order to increase their lifespan diffusion of these gases must be prevented [11]. When considering gas and moisture barriers, atomic layer deposition is an ideal deposition method. Due to the self terminating reactions of ALD, conformal and pinhole-free films can be grown even on complex and porous substrates [12, 13]. It is also possible to deposit the ALD-films at low temperatures required by the organic substrates. Therefore coating polymers with the ALD is an attractive option.

ALD thin films often contain significant amounts of hydrogen, especially when grown at low deposition temperatures. In addition to water vapour [4] and oxygen [6], also hydrogen can cause degradation for example in capacitors components [14]. Al_2O_3 thin films along with other ALD-oxides have

26 been studied as H₂ barriers for this purpose and it has been shown that the
27 diffusion of hydrogen to a capacitor dielectric material decreases significantly
28 if a protective ALD film is applied [15]. However, in some applications hy-
29 drogen is a desirable element in the film. Hydrogen from the ALD capping
30 film can, for example, passivate the Si-interface in solar-cells by binding to
31 dangling bonds which are responsible for the charge carrier recombination
32 resulting in suboptimal energy conversion efficiency [16].

33 Metal-organic ALD precursors are frequently used and the organic ligands
34 very often contain hydrogen. In addition, hydrogen containing coreactants
35 such as ¹H₂O and NH₃ are extensively used for depositing oxides and nitrides,
36 respectively. Therefore hydrogen is a common impurity in all thin films
37 but it is quite often disregarded because only a few measuring techniques,
38 such as elastic recoil detection analysis (ERDA) and secondary ion mass
39 spectrometry (SIMS), can directly detect hydrogen atoms in the films. The
40 advantage of ERDA and especially time-of-flight ERDA (ToF-ERDA) over
41 SIMS is the possibility of quantitative elemental depth profiling [17].

42 For example in the case of TMA and ¹H₂O process both precursors contain
43 hydrogen that can be incorporated in the film. Al₂O₃ can be deposited from
44 the TMA and water at as low as 33 °C but the impurity contents are then
45 very high [18]. In order to decrease the residual hydrogen concentration in
46 Al₂O₃ films, one can increase the deposition temperature [19]. Alternatively,
47 post deposition annealing can also be used to decrease the hydrogen content
48 [20]. On the other hand, many of the applications requiring gas barriers
49 involve polymers or other organic substrates and elevated temperatures can
50 not be used during or after the deposition.

51 The use of precursors containing rare stable isotopes can give information
52 not only on reaction mechanism but also on sources of impurities in the
53 films. For example, hydrogen has two stable isotopes, ^1H (99.985 %) and ^2H
54 (0.015 %) [21] and in the following text hydrogen refers to ^1H and deuterium
55 to ^2H . Similarly, water refers to $^1\text{H}_2\text{O}$ and heavy water to $^2\text{H}_2\text{O}$.

56 Deuterated precursors have been used in various studies [9, 19, 22, 23].
57 By using heavy water instead of water in TMA + $^1\text{H}_2\text{O}$ process the source
58 of hydrogen impurity can be detected. It is often presumed that as the
59 elements do not change, heavy water can be treated as equivalent to normal
60 water [9, 24, 25].

61 These isotope studies have given detailed information on reaction mecha-
62 nism and TMA + H_2O process [9, 19, 25] is probably the most widely studied
63 ALD process. That said, even the reason of the most important aspect of
64 ALD – the self terminating reaction – in the case of this process is still under
65 debate. Saturation of the reaction is often contributed to the steric hin-
66 drance of the ligands which populate the surface so that the reactive sites
67 are blocked [9, 26]. On the other hand, Vandalon *et al.* propose that the
68 steric hindrance can not be the sole cause of terminating reaction. Their
69 claim is that non-reactive methyl groups cause reactions to stop at least in
70 the lower temperatures [25]. However, there are open questions such as why
71 the persistent $-\text{CH}_3$ groups are not incorporated in the film as a carbon im-
72 purity since the deposited films contain only a small concentration of carbon
73 even at low deposition temperatures [25, 27].

74 In this work we studied how hydrogen is incorporated in the films. In
75 addition, the migration of hydrogen (and oxygen) in the films is studied. In

76 order to do so, both heavy water ($^2\text{H}_2\text{O}$) and oxygen-18 (natural abundance
77 0.2 % [21]) enriched water ($\text{H}_2\ ^{18}\text{O}$) were used as oxygen sources. The effect
78 of different ALD conditions, such as the deposition temperature and purge
79 lengths, were also studied. It was found that the impurities decrease with
80 increasing deposition temperature. In addition, the migration of hydrogen
81 was only detected if hydrogen concentration in the film was high.

82 2. Experimental details

83 Al_2O_3 films were deposited using Beneq TFS 200 side flow reactor. Ni-
84 trogen from Inmatec PN 1150 nitrogen generator (99.999 %) was used as
85 a carrier gas as well as for purging between the precursor pulses. Pressure
86 during the deposition in the reaction chamber was 1–2 mbar. TMA (Strem
87 > 98 %) was used as an aluminium source for the process. Three types
88 of water were used as an oxygen source: normal water $^1\text{H}_2^{16}\text{O}$, heavy water
89 $^2\text{H}_2^{16}\text{O}$ (Medical Isotopes Inc. 99.99 %) and oxygen-18 enriched water $^1\text{H}_2^{18}\text{O}$
90 (Medical Isotopes Inc. 97 %). Deposition temperature was varied between
91 70 °C and 250 °C. Pulse lengths for both precursors were kept constant at
92 300 ms which is double the time for our typical Al_2O_3 processes. The longer
93 pulse length was used to ensure a complete saturation of the substrate sur-
94 faces. Purging time was in most depositions 10 s after both precursor pulses
95 but the effect of the purging time was also investigated and then it was
96 varied between 3 and 60 seconds. All films were deposited on n-type (100)
97 silicon chips cut from a bigger wafer with native SiO_x layer. Sample pieces
98 were distributed in front, back and sides of the reactor in order to ensure
99 film conformality all over the reactor. To minimise H-contamination prior

100 the TMA + $^2\text{H}_2\text{O}$ deposition, the reactor was treated with 50 $^2\text{H}_2\text{O}$ pulses
101 (150 ms).

102 As-deposited samples were also exposed to elevated temperature and hu-
103 mid conditions by storing them in a climate chamber (Weiss WK3-180/40)
104 for 24 or 48 hours at 60 °C and in 80 % relative humidity (RH) at atmospheric
105 pressure.

106 The elemental composition and depth profiles of the films were mea-
107 sured with a time-of-flight elastic recoil detection analysis (ToF-ERDA) using
108 11.915 MeV $^{63}\text{Cu}^{6+}$ ions [28]. Recoiled species were detected at 41° angle us-
109 ing mirror measuring geometry. Analysis and elemental depth profiles were
110 made with Potku analysis software [29]. Surface and interface regions of
111 the films were excluded from the elemental analysis and compositions were
112 calculated from the bulk of the film.

113 Al_2O_3 films were investigated with helium ion microscopy (HIM) (Zeiss
114 Orion Nanofab) in order to study the porosity of the films.

115 Thicknesses of the films were measured with Rudolph AUTO EL III el-
116 lipsometer with 632.8 nm laser.

117 3. Results and Discussion

118 The deposition rate decreases about one third when normal water is
119 changed to $^2\text{H}_2\text{O}$ as seen in the Fig. 1a when every other parameter is kept
120 constant. Similar decrease in growth-per-cycle (GPC) is reported by Hiraiwa
121 *et al.* [24]. This is most probably due to the kinetic isotope effect, which is
122 utilised for example in chemical reaction mechanism studies [30]. This effect
123 raises the activation energy of the reaction and therefore reduces the reac-

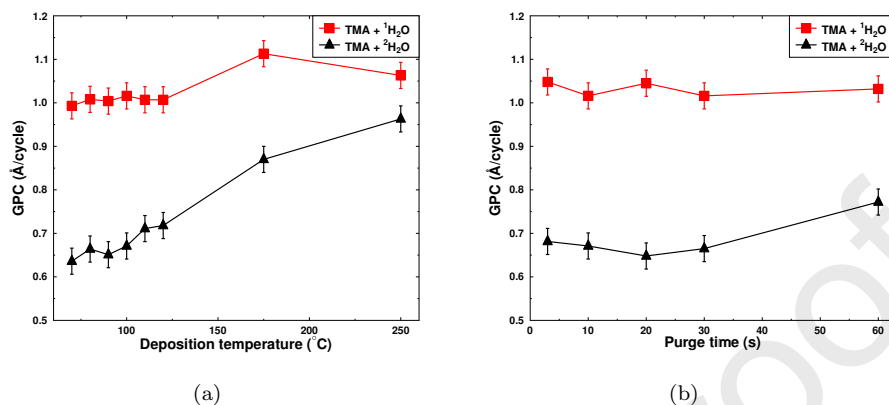


Figure 1: a) Growth-per-cycle as a function of the deposition temperature. Films were deposited using 300 ms precursor pulses and 10 s N_2 purges between the pulses. b) Growth-per-cycle of the films deposited at 100 °C. Nitrogen purge was varied between 3 and 60 s.

124 tion rate which could explain the results. As mentioned in the Introduction,
 125 the interchangeability of $^1\text{H}_2\text{O}$ and $^2\text{H}_2\text{O}$ is often assumed. On the other
 126 hand, one can not rule out that the changes in activation energies can also
 127 change the probabilities of different reaction paths making some paths more
 128 favourable than others compared to situation with normal water. For exam-
 129 ple reaction with the TMA and oxygen bridge site (i.e. Al–O–Al) [31] does
 130 not involve deuterium which may favour this reaction route if the reaction
 131 rate with O^2H -groups is decreased.

132 The GPC of the TMA + $^1\text{H}_2\text{O}$ process has been reported to increase as
 133 a function of the deposition temperature having the highest GPC at 200–
 134 300 °C depending on the source [22, 24, 32, 33]. Our results are comparable
 135 and the growth rate starts to decrease between 200 and 250 °C (Fig. 1a). This
 136 has been attributed to the decrease of reactive OH-sites due to dehydration

137 [25, 33]. On the other hand, deposition with $^2\text{H}_2\text{O}$ changes the situation so
138 that the growth rate continues to increase even at 250 °C and approaches then
139 the GPC of the $^1\text{H}_2\text{O}$ process. It seems that the extra energy from the higher
140 temperature drives the reaction more than what the dehydration slows it.
141 When considering purging times (Fig. 1b), it seems that the purging length
142 does not play a significant role in $^1\text{H}_2\text{O}$ process at 100 °C, but longer purging
143 increases the GPC slightly in $^2\text{H}_2\text{O}$ process. This is another indication of
144 slower reaction rates due to the isotope effect.

145 Composition and elemental depth profiles of the samples were produced
146 from coincidence time-of-flight and energy data (Fig. 2). Elemental com-
147 position of all the samples can be found in Supplementary (Table A.1 and
148 A.2).

149 Al_2O_3 films grown at low temperatures tend to have oxygen rich com-
150 position and the O/Al ratio closes to the stoichiometric value of 1.5 only at
151 200 °C and above [9, 18, 34]. Our similar results are shown in Fig. 3a. Also
152 purging time changes the O/Al ratio of films deposited at 100 °C (Fig. 3b)
153 although even the 60 s long purging time produces O-rich film. Even though
154 the GPC decreases when the oxygen source is changed from $^1\text{H}_2\text{O}$ to $^2\text{H}_2\text{O}$
155 (Fig. 1a), it does not affect the ratio between the main components of the
156 film. In this regard, using $^2\text{H}_2\text{O}$ instead of $^1\text{H}_2\text{O}$ is well justified.

157 While O/Al ratio is independent of the oxygen precursor, there is a dif-
158 ference in the amount of hydrogen incorporated in the films (Fig. 4a). Films
159 deposited with heavy water tend to have slightly higher total amount of ^1H
160 and ^2H compared to hydrogen content in the films deposited with normal wa-
161 ter. In earlier studies the equivalence between the use of $^1\text{H}_2\text{O}$ or $^2\text{H}_2\text{O}$ have

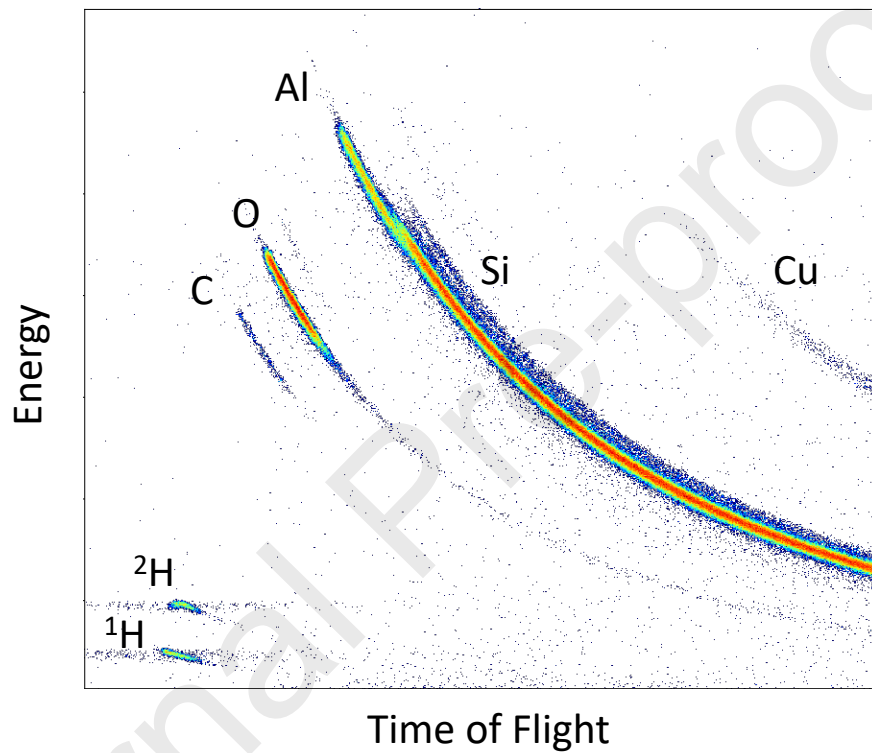


Figure 2: Coincidence time-of-flight and energy histogram of a ToF-ERDA measurement. Elements and isotopes differentiate according to their masses. Film was deposited using 1000 cycles of TMA and $^2\text{H}_2\text{O}$ at 100 °C. Scattered ^{63}Cu beam used for the measurement is also visible.

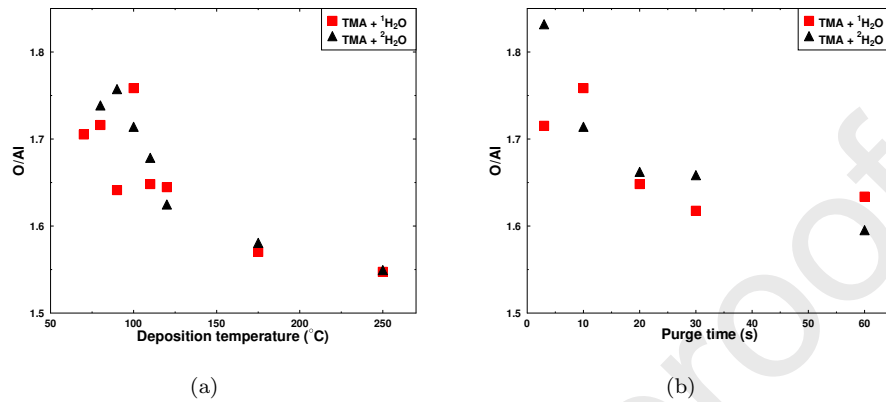


Figure 3: a) O/Al ratio as a function of the deposition temperature. Samples were deposited using 300 ms precursor pulses and 10 s purging. b) O/Al ratio as a function of the purging time. Samples were deposited at 100 °C.

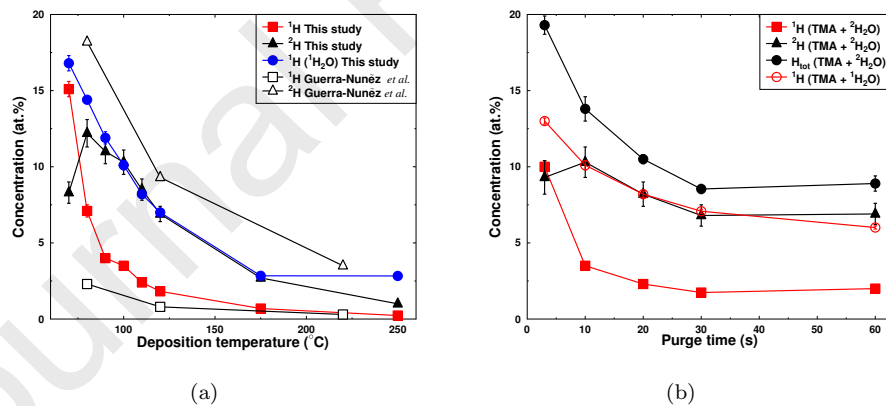


Figure 4: a) ^1H and ^2H impurity concentrations at different deposition temperatures. Films were deposited using 300 ms precursor pulses and 10 s purging times. Comparison to Guerra-Nunéz *et al.* [9] is also shown. b) ^1H and ^2H concentrations as a function of purge time. Deposited at 100 °C using 300 ms precursor pulses.

162 been justified by similar total hydrogen concentrations [9, 19]. Somewhat
163 similar results to ours, with higher total hydrogen when $^1\text{H}_2\text{O}$ was replaced
164 with $^2\text{H}_2\text{O}$, were obtained by Hiraiwa *et al.* [24]. However, their conclusion
165 was that the difference is not significant and can be neglected. Nevertheless,
166 the total hydrogen concentration follows a similar trend with both oxygen
167 precursors even though the use of $^2\text{H}_2\text{O}$ results in somewhat higher total
168 hydrogen concentration than $^1\text{H}_2\text{O}$.

169 The deposition temperature plays a major role in hydrogen incorporation
170 in ALD- Al_2O_3 films. At high temperatures the hydrogen concentration de-
171 creases as shown in Fig. 4a and goes below 5 at. % only above 175 °C. The
172 main hydrogen source is from water since there is more deuterium than hy-
173 drogen in the film when the deposition temperature is higher than 70 °C. It
174 is notable that in our study the majority hydrogen isotope changes from hy-
175 drogen to deuterium between 70 and 80 °C. Films deposited at 70 °C, based
176 on visual inspection as well as with thickness profiles given by the ellipsome-
177 ter, appeared completely fine; films were uniform in thickness all around
178 the reactor and visually looked similar to ones deposited at higher tempera-
179 tures. When the deposition temperature was decreased to 60 °C clear signs of
180 CVD-growth were observed (See Supplementary A.7) for the TMA + $^2\text{H}_2\text{O}$
181 process. Films deposited with $^1\text{H}_2\text{O}$ were uniform. The drastic change in ^1H
182 and ^2H composition at 70 °C would therefore be an indication of CVD com-
183 ponent in the reaction. It is known [18] that water molecules physisorpt to
184 "cold" surfaces and require long pumping (i.e. purging) time. If the purging
185 time is not sufficient, physisorption leads to higher than monolayer surface
186 concentration of $^1\text{H}_2\text{O}$ or OH which is still present when TMA is pulsed to

187 the reactor. However, as seen in Fig. 4a, the deuterium concentration drops
188 significantly at 70 °C, indicating that deuterium from water is not incorpo-
189 rated in the film in large quantities. In addition, CVD-growth would increase
190 the GPC which was not observed at 70 °C (Fig. 1a). This can be explained
191 by the studies of Vandalon *et al.* [22, 25] where they showed that there is
192 a certain temperature limit where water is not reactive enough towards the
193 CH₃-groups at the substrate surface which leaves excessive amount of persis-
194 tent CH₃-groups in the film. As Vandalon *et al.* pointed out, also simulations
195 suggest that the isolated CH₃-groups have higher reaction barrier compared
196 to the multiple methyl groups in close proximity to each other [35]. These
197 isolated unreactive methyl groups could be the source of the high hydrogen
198 concentration in the film deposited at 70 °C.

199 As seen in Fig. 5a and 5b, the carbon concentration follows very similar
200 trend to the hydrogen concentration and decreases with the increasing depo-
201 sition temperature and purge length. Carbon concentration is not high even
202 at low temperatures and the use of ²H₂O instead of ¹H₂O does not have a
203 significant effect on carbon concentration. However, it remains as an open
204 question what happens to the carbon since even at 70 °C the amount of
205 carbon in the films is only 2.3±0.2 at.% (Fig. 5a). If hydrogen would be in
206 the film in the form of methyl groups we should expect carbon concentration
207 to be closer to 5 at.%. Same observation was done by Vandalon *et al.* and
208 they proposed that these methyl groups can react with water in subsequent
209 cycles.

210 Comparison of ¹H and ²H impurities with previous work by Guerra-Nunéz
211 *et al.* is made also in Fig. 4a. General trends are similar although our

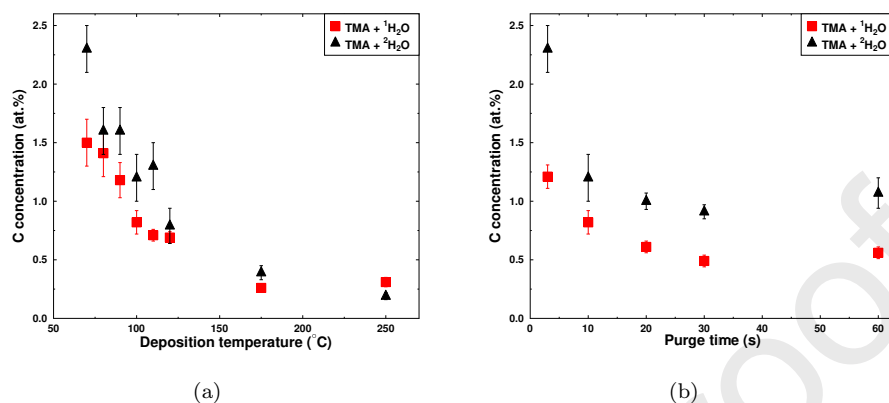


Figure 5: a) Carbon concentration of films deposited at different temperatures using 300 ms pulses and 10 s purging times. b) Carbon concentration as a function of purging times, films were deposited at 100 °C using 300 ms pulses.

212 results show slightly higher deuterium content but somewhat lower hydrogen
 213 incorporation. All our samples in Fig. 4a are deposited with 300 ms precursor
 214 pulses and 10 s N₂ purges while Guerra-Nun̄ez *et al.* used 1 s pulses, 2 s
 215 exposure time and 60 s purging. While this long ALD cycle can improve the
 216 film quality, it also makes the deposition very long and maybe impractical
 217 for industrial purposes.

218 The length of the purge has a significant effect on the hydrogen incor-
 219 poration in the film as seen in Fig. 4b. Both the hydrogen and deuterium
 220 concentration decrease as the purging times increases. Although deposited
 221 films are conformal in thickness (less than 2 % variation over the area of
 222 the reactor) even with the shorter purging times, and therefore seem to rep-
 223 resent pure and self-limiting ALD-growth, the films are far from identical.
 224 Reactions are observed to go to completion at quite slow rate at low temper-
 225 atures, requiring 30 s purging even as high as at 100 °C before the hydrogen

226 concentration saturates. Similar trend is observed for $^1\text{H}_2\text{O}$ process which is
227 somewhat surprising since the GPC does not change with increasing purging
228 times (Fig. 1b).

229 The mass gain per cycle is a more direct indication of slow reaction rate
230 and desorption of reaction species at low temperatures compared to measur-
231 ing only GPC, as films with similar thickness can have different mass density.
232 It is shown on quartz crystal microbalance (QCM) studies that the mass gain
233 per cycle decreases as the purging times are increased at low temperatures
234 [18, 36]. In addition, the mass loss after the precursor pulse can continue for
235 tens of seconds indicating that the reactions are slow and the desorption of
236 reaction products and physisorbed surface species require long purging times
237 at low temperatures. This supports our finding that long purging times de-
238 crease hydrogen, carbon and excess oxygen content in the film.

239 This purging time issue is one example of a sources of inconsistency in
240 ALD research pointed out by Sønsteby *et al.* in the recent paper [37]. They
241 address the problems on ALD reproducibility and relate, for example, higher
242 than expected GPC to short purging times possibly leading to CVD like
243 growth. This is all true, but looking only at the GPC does not guarantee
244 that the results are comparable as we have shown above. Even if purging
245 times are adequate to produce conformal films, purging can be short enough
246 to also change the composition of the film as seen in Figure 4b even if the GPC
247 does not change (See Fig. 1b). In addition, the reactor used will influence the
248 required purging (and pulsing) times. Details, such as vacuum level, reactor
249 geometry and gas flows will have an effect on deposition and film growth. It
250 is important to note this issue when comparing the results obtained by the

251 different groups. This issue is most pronounced at low temperatures. As seen
252 in Fig. 4a, our results are somewhat different compared to those measured
253 by Guerra-Nun ez *et al.* The difference between our and their results is of
254 order of a few at.% which is larger than the margin of error. Therefore
255 the discrepancy must come from the different pulsing and purging times,
256 reactor geometry and deposition pressure, and it is important to report all
257 the deposition parameters in order to compare the results reliably.

258 We also studied the hydrogen migration in the Al₂O₃ films. A depth
259 profile of an as-deposited TMA + ²H₂O film is presented in Figure 6a).
260 The films were deposited using 150 ms precursor pulses and 3 s purging
261 at 100 °C which makes them hydrogen rich. In figure 6b) the same film
262 is shown after 24 h exposure in a climate chamber. The conditions in the
263 chamber were kept constant at 60 °C and at 80 % relative humidity. After
264 the treatment the deuterium concentration was dramatically decreased and
265 at the same time the concentration of ¹H had increased equally keeping the
266 total amount of elemental hydrogen constant. This can be explained by the
267 hydrogen exchange reactions. Hydrogen in water vapour and gaseous H₂ can
268 exchange hydrogen atoms with the impurity hydrogen/deuterium in the film.
269 Since the natural abundance of deuterium (0.02 %) is much lower than the
270 ratio in these films, the percentage of the ²H drops due to these exchanges.
271 Interestingly, the exchange does not happen only at the surface but also all
272 the way through the 80 nm thick films. This requires migration of hydrogen
273 for rather long distances even in these low temperature annealing conditions.
274 Other possibility is that the film is porous and gases penetrate the film easily.
275 However, there is a threshold for hydrogen concentration that is needed

276 for the exchange reaction to proceed through the whole film. Sample de-
277 posited at 100 °C with 300 ms pulses and 10 s purging times contain ~ 15 at.%
278 of total hydrogen ($^1\text{H} + ^2\text{H}$). When this sample is exposed to climate cham-
279 ber conditions, there are no major changes in either hydrogen or deuterium
280 concentrations (See Supplementary A.9).

281 We can observe in Fig. 6a that both ^1H and ^2H are unevenly distributed
282 in the film. There is more ^1H at the surface and more ^2H at the interface.
283 This is an example of a similar exchange reaction that happens also at room
284 temperature in air given enough time (1 day) between the deposition and
285 characterization (see Supplementary Fig. A.8). Therefore data shown in
286 Figures 1, 3, 4 and 5 were measured from the samples that were kept in a
287 load-lock under a vacuum condition (< 1 mbar) until exposed to air very
288 briefly just before the characterization.

289 It is known based on IR-studies that the hydrogen impurities in ALD-
290 Al_2O_3 films are found at least in the form of OH-groups [38, 39]. Signal from
291 OH stretching has been shown to increase as the hydrogen content of the film
292 increases, supporting the claim that hydrogen is found in the films in form
293 of OH-groups [38]. Films deposited at low temperature are also oxygen rich
294 hinting that there are undercoordinated oxygen atoms. Relatively low carbon
295 concentration rules out the speculation that the majority of the hydrogen
296 would be in the form of CH_3 -groups. Furthermore, in the films grown with
297 $\text{TMA} + ^2\text{H}_2\text{O}$, ^2H atoms are most likely bound to oxygen as they originate
298 from the water.

299 In order to see if the hydrogen migration is related to the movement
300 of the whole OH-group or if there is any oxygen diffusion from the ambient

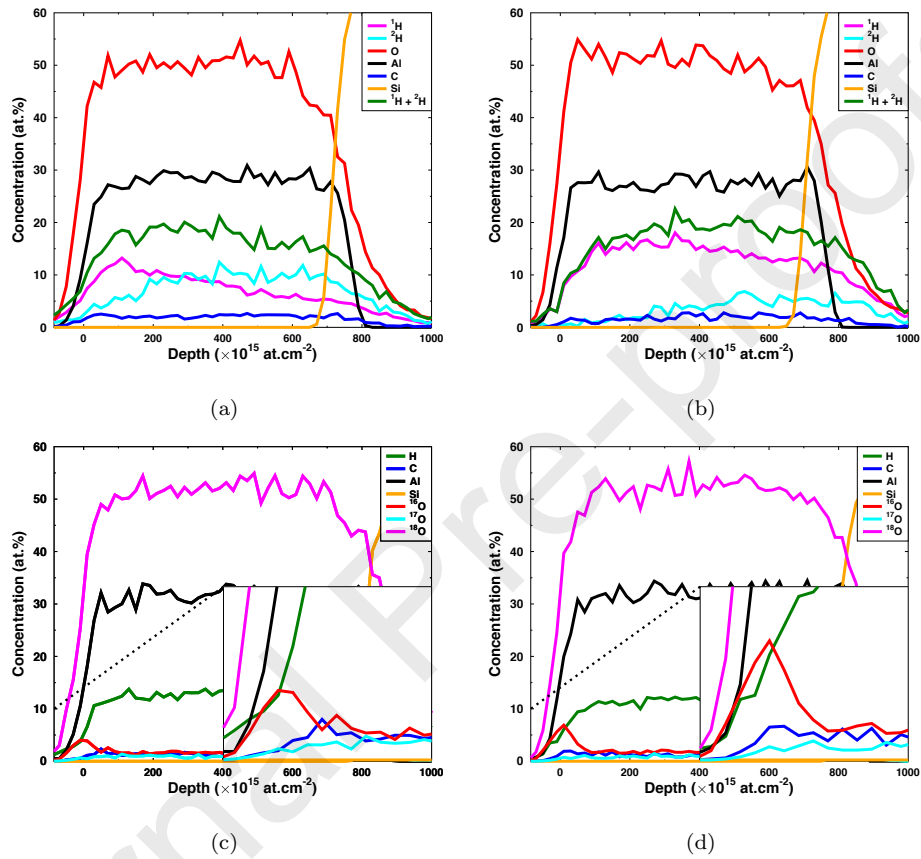


Figure 6: Elemental depth profiles of Al_2O_3 films deposited at 100 °C with 150 ms precursor pulses and 3 s purging. a) As-deposited film using TMA and $^2\text{H}_2\text{O}$. The sample was kept at room temperature in air for one day before the characterization. b) The same film as in a) but after 24 h at 60 °C and 80 % RH. c) As-deposited film using TMA and H_2^{18}O . The sample was kept for one day at room temperature in air before the characterization. d) The same film as in c) but after 48 h in 60 °C and 80 % RH.

301 present, films using TMA and H_2^{18}O as precursors were deposited. The depth
302 profile of an as-deposited film grown at 100 °C is presented in Fig. 6c). We
303 see that oxygen-18 enriched water produces films that contain less hydrogen
304 than the films deposited with $^2\text{H}_2\text{O}$. However, hydrogen concentration in Fig.
305 6c is comparable to the samples deposited with $^1\text{H}_2\text{O}$. This is expected since
306 small change in oxygen mass does not have a great effect on the activation
307 energy and therefore kinetic isotope effect is not noticeable. After 48 h in
308 the climate chamber at 60 °C and at 80 % RH the films show only very
309 minor difference at the surface as seen in Figure 6d). Inside the film the
310 amount of oxygen-18 does not change, indicating that oxygen even in OH-
311 groups can not efficiently exchange with oxygen from O_2 or H_2O at similar
312 rate compared to hydrogen. This indicates that only hydrogen is migrating
313 in the film, not whole OH-groups. From the results it is also clear that the
314 oxygen that is bonded to aluminium does not exchange with oxygen atoms
315 from O_2 or $^1\text{H}_2\text{O}$ molecules.

316 Dingemann *et al.* showed that hydrogen effuses from the Al_2O_3 films in
317 the form of both H_2 and $^1\text{H}_2\text{O}$ when annealed at 200 to 1000 °C in high
318 vacuum (10^{-7} mbar) conditions [20]. That process, however, must be dif-
319 ferent compared to process reported in this paper. The high temperature
320 annealing removes and so decreases the amount of hydrogen in the films.
321 Here we observe only an (isotope) exchange reaction and the total amount of
322 hydrogen in the film does not change. Considering that the $^1\text{H}/^2\text{H}$ -exchange
323 reaction is chemically similar to the H/H-exchange, it is clear that the hy-
324 drogen moves through the films easily if the film has been deposited at low
325 temperature and has high hydrogen content. Hydrogen diffusion studies done

326 by Cameron *et al.* with radioactive hydrogen isotope tritium (^3H) show that
327 hydrogen can diffuse through also in atomic form [40], which is in agreement
328 with our findings.

329 Porosity of the film could increase both the efficiency of the hydrogen
330 exchange and hydrogen permeation in the film enabling gases to penetrate
331 and interact also deeper in the film. Many amorphous ALD films are known
332 to be pinhole free [4, 41] and this was confirmed also here with helium ion
333 microscopy (HIM) (See Supplementary A.10a and A.10b). With the nominal
334 HIM resolution of 0.5 nm no detectable porosity could be observed.

335 4. Conclusions

336 Although ALD alumina films have been suggested and used as possible
337 gas barriers, it is clear that at least hydrogen is able to transport through the
338 film rather easily in a warm and humid environment if the initial hydrogen
339 concentration of the film is high. Our results indicate that the hydrogen
340 transport proceeds via hydrogen exchange reactions. Therefore it is possible
341 to decrease the hydrogen transport by controlling the amount of hydrogen left
342 in the film during the deposition. This can be achieved by careful selection
343 of precursors or increasing the deposition temperature and using very long
344 purging times. Optionally also post-deposition annealing can be applied.
345 However, the coated material in barrier applications is commonly a polymer,
346 which many times rules out high deposition temperatures. Longer purges
347 in turn increase the deposition times, possibly by an order of magnitude,
348 which reduces the throughput significantly making the ALD- Al_2O_3 films as
349 hydrogen permeation barriers not so attractive method.

350 As demonstrated here, a significant amount of hydrogen is stored in the
351 films and hydrogen can also move through the film if the concentration is
352 high. Oddly enough, this could open opportunities using ALD- Al_2O_3 films as
353 proton conductors [42]. ALD also offers various ways to control the hydrogen
354 content and diffusion.

355 In order to study the hydrogen incorporation in the films, we replaced
356 $^1\text{H}_2\text{O}$ with $^2\text{H}_2\text{O}$. Change of isotope in a molecule should not change the
357 chemistry since the element is not changed. However, in the case of hydrogen,
358 replacing hydrogen with deuterium doubles the mass of the atom and it
359 affects the film growth. Growth per cycle is decreased and impurity carbon
360 and total hydrogen incorporated in the film is increased when $^2\text{H}_2\text{O}$ is used.
361 On the other hand, the ratio between the main components, oxygen and
362 aluminium, is independent of oxygen precursor. While there are differences
363 in the films depending on the oxygen precursor, the general trends are similar
364 and therefore the comparison is justified when done carefully.

365 It is also noteworthy to keep in mind that in addition to pulsing times
366 and deposition temperature, purging times affect greatly the film quality and
367 this should be taken in to account especially when comparing results from
368 different studies. Our work clearly demonstrates that even though a quick
369 glance at the samples does not show any difference, there can be a significant
370 difference in the compositions. If this is the case even with the close to
371 "ideal" ALD process of TMA and water, even more care should be taken
372 when interpreting results obtained with limited characterization techniques
373 from more demanding processes.

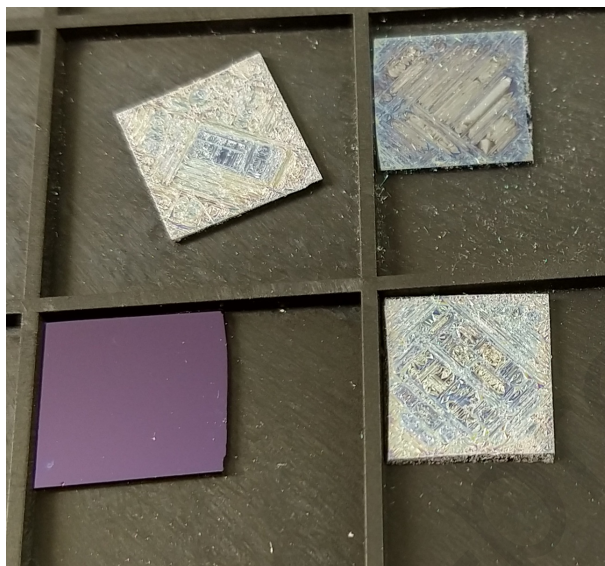


Figure A.7: Uncontrolled CVD-growth on three silicon chips (TMA + $^2\text{H}_2\text{O}$) and one sample with proper film (TMA + $^1\text{H}_2\text{O}$). All samples were deposited at 60 °C with 300 ms pulses and 10 s purging.

374 **Appendix A. Supplementary**

375 When the purging times are too short and there is a substantial amount of
376 previous precursor available when the next precursor is introduced to reactor,
377 growth is not under control and we experience CVD-like growth (Fig. A.7).
378 The film is also much thicker than what would be expected for the ALD-
379 growth.

380 If films are not properly stored, the hydrogen exchange reactions take
381 place also at room temperature as seen in Fig. A.8. As the concentration of
382 deuterium decreases over time, the concentration of hydrogen increases. The
383 total amount of $^1\text{H} + ^2\text{H}$ increases slightly but the change is not significant.

384 However, there seems to be a threshold value for hydrogen exchange re-

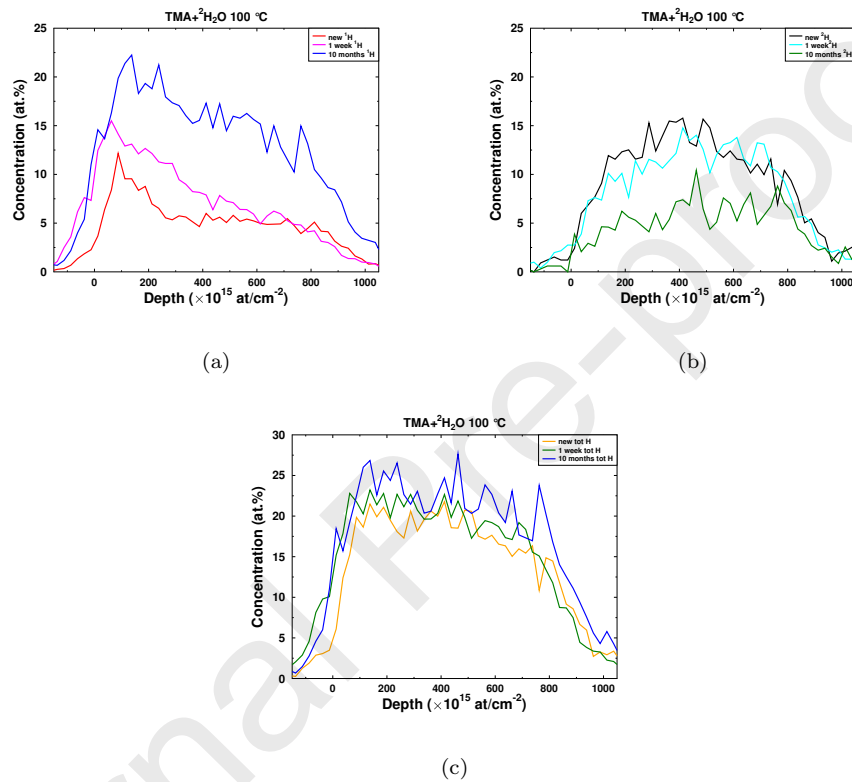


Figure A.8: The sample was deposited at 100 °C using 150 ms pulses and 3 s purging making the hydrogen concentration high. The sample was stored in ambient condition and measured again later. The ^1H concentration increased as the ^2H concentration decreased equally. a) Elemental depth profile of ^1H , b) ^2H and c) the sum of ^1H and ^2H presented in a) and b).

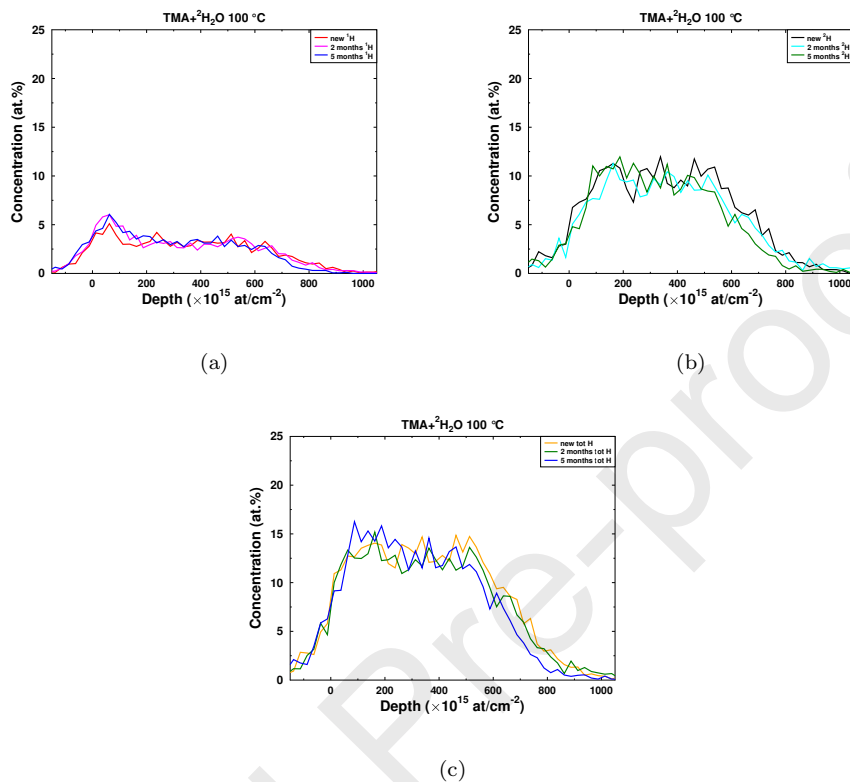


Figure A.9: The sample was deposited at 100 °C using 300 ms pulses and 10 s purging and was stored in ambient conditions and measured again later. a) Elemental depth profile of ¹H, b) ²H and c) the sum of ¹H and ²H presented in a) and b).

385 action. If longer purging times are used, resulting lower hydrogen content,
 386 there is no significant change in hydrogen or deuterium content when samples
 387 are stored in air as seen in Fig. A.9.

388 The cross section of an Al₂O₃ film is seen HIM micrograph (Fig A.10)
 389 tilted in 30° angle. Micrograph shows a pinhole free surface. However, HIM
 390 does not resolve any sub-nanometer porosity.

391 In Table A.1 are listed the elemental compositions of the films in tem-

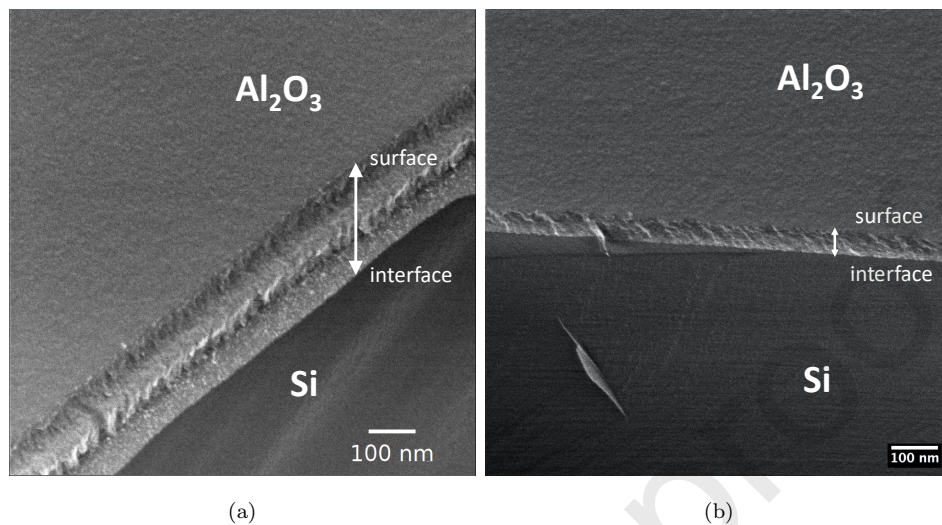


Figure A.10: Cleaved 100 nm thick Al_2O_3 film at 30° angle imaged with HIM. a) The film was deposited with TMA and $^2\text{H}_2\text{O}$ at 100°C using 150 ms precursor pulses and 3 s purging. b) The film was deposited with same recipe as in a) but using TMA + $^1\text{H}_2^{18}\text{O}$.

392 perature series and in Table A.2 are the elemental compositions of the films
 393 deposited at 100°C with varying purge lengths.

Table A.1: Elemental composition of the films deposited at different temperatures. The films were deposited using TMA and $^1\text{H}_2\text{O}/^2\text{H}_2\text{O}$ with 300 ms pulses and 10 s purging.

TMA + $^2\text{H}_2\text{O}$					
T(°C)	Al	O	C	^1H	^2H
70	25.9±0.6	48.5±0.9	2.3±0.2	15.1±0.5	8.3±0.7
80	28.9±0.7	50.2±1	1.6±0.2	7.1±0.4	12.2±0.9
90	30.3±0.7	53.2±1	1.6±0.2	4±0.2	11±0.8
100	31.3±0.7	53.6±1	1.2±0.2	3.5±0.2	10.3±0.8
110	32.8±0.7	55±1	1.3±0.2	2.4±0.2	8.5±0.7
120	34.5±0.6	56±0.9	0.79±0.11	1.82±0.15	6.9±0.5
175	37.3±0.4	58.9±0.6	0.39±0.05	0.69±0.06	2.7±0.2
250	38.7±0.4	59.9±0.6	0.19±0.03	0.23±0.03	1±0.13
TMA + $^1\text{H}_2\text{O}$					
70	30.2±0.6	51.5±0.9	1.5±0.2	16.8±0.5	-
80	31±0.3	53.2±0.4	1.41±0.07	14.4±0.2	-
90	32.9±0.7	54±0.9	1.18±0.15	11.9±0.4	-
100	32.3±0.5	56.8±0.8	0.82±0.1	10.1±0.3	-
110	34.4±0.2	56.7±0.3	0.71±0.04	8.2±0.11	-
120	34.9±0.3	57.4±0.4	0.69±0.05	7±0.14	-
175	37.7±0.3	59.2±0.5	0.26±0.03	2.84±0.1	-
250	38±0.3	58.8±0.5	0.31±0.04	2.83±0.1	-

Table A.2: Elemental composition of the films deposited with different purging times. The films were deposited using TMA and $^1\text{H}_2\text{O}/^2\text{H}_2\text{O}$ with 300 ms pulses at 100 °C.

TMA + $^2\text{H}_2\text{O}$					
Purge (s))	Al	O	C	^1H	^2H
3	27.7±0.6	50.7±0.8	2.3±0.2	10±0.4	9.3±0.6
10	31.3±0.7	53.6±1.0	1.2±0.2	3.5±0.2	10.3±0.8
20	33.3±0.3	55.3±0.5	1±0.07	2.3±0.09	8.2±0.3
30	34.1±0.3	56.5±0.4	0.91±0.06	1.74±0.07	6.8±0.3
60	34.7±0.6	55.3±0.9	1.07±0.13	2±0.13	6.9±0.5
TMA + $^2\text{H}_2\text{O}$					
3	31.6±0.2	54.2±0.3	1.21±0.05	13±0.2	-
10	32.3±0.5	56.8±0.8	0.82±0.1	10.1±0.3	-
20	34.4±0.3	56.7±0.5	0.61±0.05	8.2±0.2	-
30	35.3±0.3	57.1±0.4	0.49±0.04	7.08±0.13	-
60	35.5±0.2	58±0.3	0.56±0.03	6.01±0.1	-

394 **References**

- 395 [1] M. Groner, J. Elam, F. Fabreguette, S. George, Electrical Characteriza-
396 tion of Thin Al₂O₃ Films Grown by Atomic Layer Deposition on Silicon
397 and Various Metal Substrates, *Thin Solid Films* 413 (2002) 186 – 197.
- 398 [2] R. Y. Khosa, E. B. Thorsteinsson, M. Winters, N. Rorsman, R. Karhu,
399 J. Hassan, E. Sveinbjörnsson, Electrical Characterization of Amor-
400 phous Al₂O₃ Dielectric Films on n-type 4H-SiC, *AIP Advances* 8 (2018)
401 025304.
- 402 [3] J. Acharya, J. Wilt, B. Liu, J. Wu, Probing the Dielectric Properties
403 of Ultrathin Al/Al₂O₃/Al Trilayers Fabricated Using in Situ Sputtering
404 and Atomic Layer Deposition, *ACS Applied Materials & Interfaces* 10
405 (2018) 3112–3120. PMID: 29293311.
- 406 [4] P. F. Carcia, R. S. McLean, M. H. Reilly, M. D. Groner, S. M. George,
407 Ca test of Al₂O₃ gas diffusion barriers grown by atomic layer deposition
408 on polymers, *Applied Physics Letters* 89 (2006) 031915.
- 409 [5] S.-H. K. Park, J. Oh, C.-S. Hwang, J.-I. Lee, Y. S. Yang, H. Y. Chu,
410 K.-Y. Kang, Ultra Thin Film Encapsulation of Organic Light Emitting
411 Diode on a Plastic Substrate, *ETRI Journal* 27 (2005) 545–550.
- 412 [6] T. Hirvikorpi, M. Vähä-Nissi, T. Mustonen, E. Iiskola, M. Karppinen,
413 Atomic Layer Deposited Aluminum Oxide Barrier Coatings for Packag-
414 ing Materials, *Thin Solid Films* 518 (2010) 2654 – 2658.
- 415 [7] AtomicLimits, ALD database, DOI:10.6100/alddatabase, 2020.

- 416 [8] V. Miikkulainen, M. Leskelä, M. Ritala, R. Puurunen, Crystallinity of
417 inorganic films grown by atomic layer deposition: Overview and general
418 trends, *Journal of Applied Physics* 113 (2013) 021301.
- 419 [9] C. Guerra-Nunéz, M. Döbeli, J. Michler, I. Utke, Reaction and growth
420 mechanisms in Al₂O₃ deposited via atomic layer deposition: Elucidating
421 the hydrogen source, *Chemistry of Materials* 29 (2017) 8690–8703.
- 422 [10] A. P. Ghosh, L. J. Gerenser, C. M. Jarman, J. E. Fornalik, Thin-
423 film Encapsulation of Organic Light-emitting Devices, *Applied Physics*
424 *Letters* 86 (2005) 223503.
- 425 [11] M. Schaer, F. Nüesch, D. Berner, W. Leo, L. Zuppiroli, Water Vapor
426 and Oxygen Degradation Mechanisms in Organic Light Emitting Diodes,
427 *Advanced Functional Materials* 11 (2001) 116–121.
- 428 [12] M. Ritala, M. Leskelä, J.-P. Dekker, C. Mutsaers, P. J. Soininen,
429 J. Skarp, Perfectly Conformal TiN and Al₂O₃ Films Deposited by
430 Atomic Layer Deposition, *Chemical Vapor Deposition* 5 (1999) 7–9.
- 431 [13] I. Iatsunskyi, M. Kempíski, M. Jancelewicz, K. Załeski, S. Jurga,
432 V. Smyntyna, Structural and XPS Characterization of ALD Al₂O₃
433 Coated Porous Silicon, *Vacuum* 113 (2015) 52 – 58.
- 434 [14] D. Sohrabi Baba Heidary, C. A. Randall, Analysis of the Degradation
435 of BaTiO₃ Resistivity due to Hydrogen Ion Incorporation: Impedance
436 Spectroscopy and Diffusion Analysis, *Acta Materialia* 96 (2015) 344 –
437 351.

- 438 [15] D. Sohrabi Baba Heidary, W. Qu, C. A. Randall, Evaluating the Merit of
439 ALD Coating as a Barrier Against Hydrogen Degradation in Capacitor
440 Components, *RSC Adv.* 5 (2015) 50869–50877.
- 441 [16] L. Black, B. van de Loo, B. Macco, J. Melskens, W. Berghuis,
442 W. Kessels, Explorative Studies of Novel Silicon Surface Passivation
443 Materials: Considerations and Lessons Learned, *Solar Energy Materials*
444 *and Solar Cells* 188 (2018) 182 – 189.
- 445 [17] S. Giangrandi, T. Sajavaara, B. Brijs, K. Arstila, A. Vantomme, W. Van-
446 dervorst, Low-energy heavy-ion TOF-ERDA Setup for Quantitative
447 Depth Profiling of Thin Films, *Nuclear Instruments and Methods*
448 *in Physics Research Section B: Beam Interactions with Materials and*
449 *Atoms* 266 (2008) 5144 – 5150.
- 450 [18] M. D. Groner, F. H. Fabreguette, J. W. Elam, S. M. George, Low-
451 Temperature Al₂O₃ Atomic Layer Deposition, *Chemistry of Materials*
452 16 (2004) 639–645.
- 453 [19] M. Juppo, A. Rahtu, M. Ritala, M. Leskelä, In situ mass spectrometry
454 study on surface reactions in atomic layer deposition of Al₂O₃ thin films
455 from trimethylaluminum and water, *Langmuir* 16 (2000) 4034–4039.
- 456 [20] G. Dingemans, F. Einsele, W. Beyer, M. C. M. van de Sanden, W. M. M.
457 Kessels, Influence of Annealing and Al₂O₃ Properties on the Hydrogen-
458 induced Passivation of the Si/SiO₂ Interface, *Journal of Applied Physics*
459 111 (2012) 093713.

- 460 [21] CIAAW, Isotopic compositions of the elements 2019. Available online at
461 www.ciaaw.org, 2020.
- 462 [22] V. Vandalon, W. M. M. Kessels, What is limiting low-temperature
463 atomic layer deposition of Al_2O_3 ? a vibrational sum-frequency genera-
464 tion study, *Applied Physics Letters* 108 (2016) 011607.
- 465 [23] G. Dingemans, W. Beyer, M. C. M. van de Sanden, W. M. M. Kessels,
466 Hydrogen Induced Passivation of Si Interfaces by Al_2O_3 Films and
467 $\text{SiO}_2/\text{Al}_2\text{O}_3$ Stacks, *Applied Physics Letters* 97 (2010) 152106.
- 468 [24] A. Hiraiwa, T. Saito, D. Matsumura, H. Kawarada, Isotope Analysis
469 of Diamond-surface Passivation Effect of High-temperature H_2O -grown
470 Atomic Layer Deposition- Al_2O_3 Films, *Journal of Applied Physics* 117
471 (2015) 215304.
- 472 [25] V. Vandalon, W. M. M. Kessels, Revisiting the Growth Mechanism
473 of Atomic Layer Deposition of Al_2O_3 : A Vibrational Sum-frequency
474 Generation Study, *Journal of Vacuum Science & Technology A* 35 (2017)
475 05C313.
- 476 [26] R. L. Puurunen, Surface Chemistry of Atomic Layer Deposition: A Case
477 Study for the Trimethylaluminum/Water Process, *Journal of Applied*
478 *Physics* 97 (2005) 121301.
- 479 [27] O. M. Ylivaara, X. Liu, L. Kilpi, J. Lyytinen, D. Schneider, M. Laiti-
480 nen, J. Julin, S. Ali, S. Sintonen, M. Berdova, E. Haimi, T. Sajavaara,
481 H. Ronkainen, H. Lipsanen, J. Koskinen, S.-P. Hannula, R. L. Puurunen,
482 Aluminum Oxide from Trimethylaluminum and Water by Atomic Layer

- 483 Deposition: The Temperature Dependence of Residual Stress, Elastic
484 Modulus, Hardness and Adhesion, *Thin Solid Films* 552 (2014) 124 –
485 135.
- 486 [28] M. Laitinen, M. Rossi, J. Julin, T. Sajavaara, Time-of-flight – Energy
487 spectrometer for elemental depth profiling – Jyväskylä design, *Nuclear*
488 *Instruments and Methods in Physics Research Section B: Beam Inter-*
489 *actions with Materials and Atoms* 337 (2014) 55 – 61.
- 490 [29] K. Arstila, J. Julin, M. Laitinen, J. Aalto, T. Konu, S. Kärkkäinen,
491 S. Rahkonen, M. Raunio, J. Itkonen, J.-P. Santanen, T. Tuovinen, T. Sa-
492 javaara, Potku – New analysis software for heavy ion elastic recoil de-
493 tection analysis, *Nuclear Instruments and Methods in Physics Research*
494 *Section B: Beam Interactions with Materials and Atoms* 331 (2014) 34 –
495 41. 11th European Conference on Accelerators in Applied Research and
496 Technology.
- 497 [30] M. Gómez-Gallego, M. Sierra, Kinetic Isotope Effects in the Study of
498 Organometallic Reaction Mechanisms, *Chemical Reviews* 111 (2011)
499 4857–4963. PMID: 21545118.
- 500 [31] R. Puurunen, M. Lindblad, A. Rootc, A. Krausea, Successive reactions
501 of gaseous trimethylaluminium and ammonia on porous alumina, *Phys-*
502 *ical Chemistry Chemical Physics* 3 (2001) 1093–1102. Cited By 76.
- 503 [32] R. Matero, A. Rahtu, M. Ritala, M. Leskelä, T. Sajavaara, Effect of
504 Water Dose on the Atomic Layer Deposition Rate of Oxide Thin Films,
505 *Thin Solid Films* 368 (2000) 1 – 7.

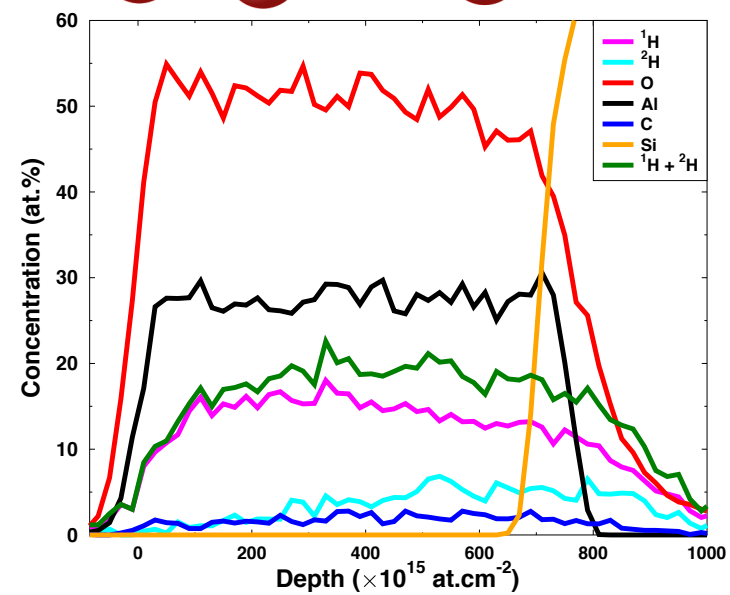
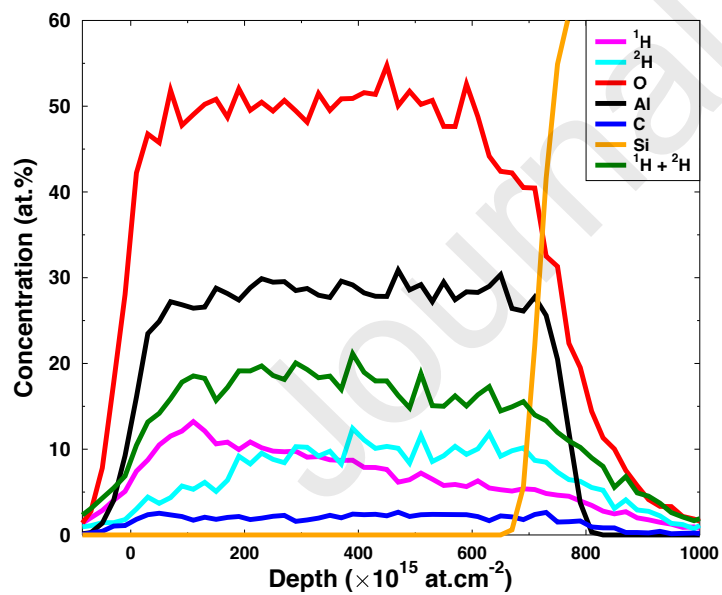
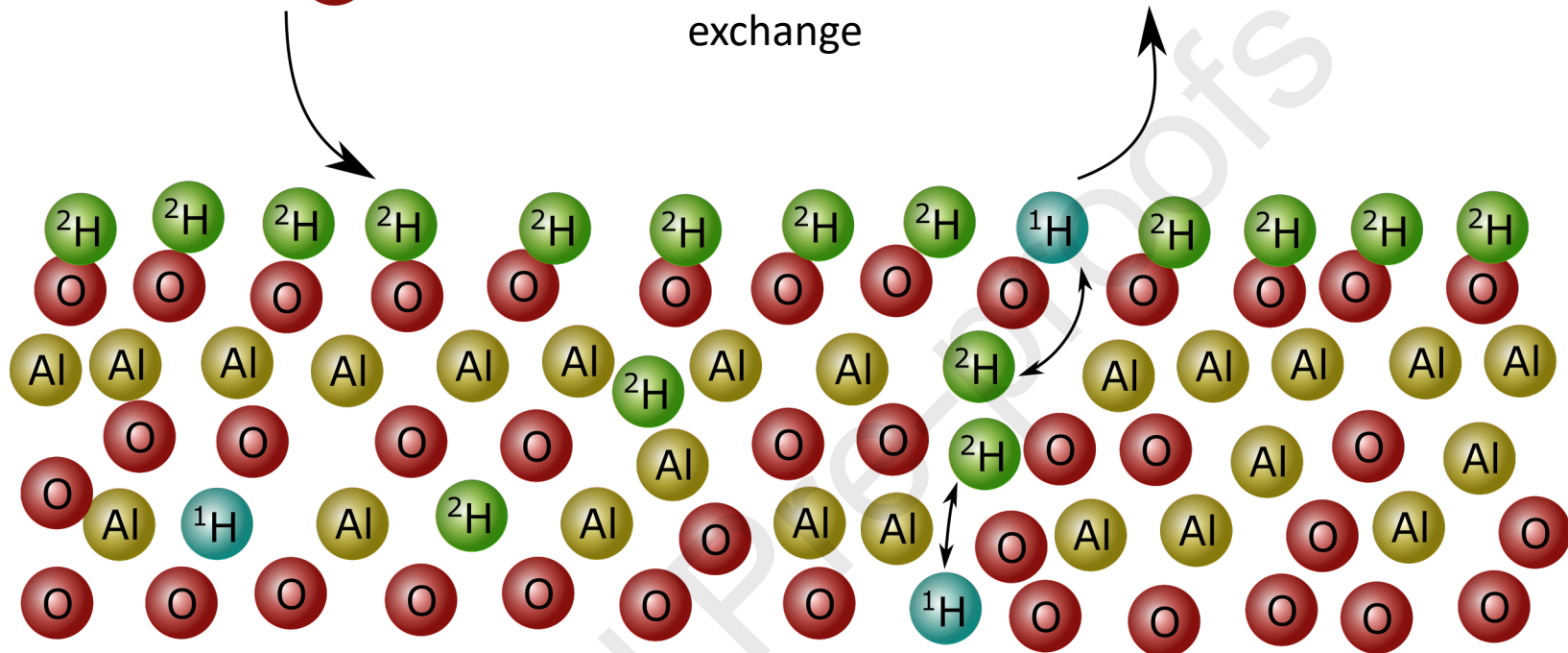
- 506 [33] G. P. Gakis, H. Vergnes, E. Scheid, C. Vahlas, A. G. Boudouvis, B. Caus-
507 sat, Detailed Investigation of the Surface Mechanisms and Their Inter-
508 play with Transport Phenomena in Alumina Atomic Layer Deposition
509 from TMA and Water, *Chemical Engineering Science* 195 (2019) 399 –
510 412.
- 511 [34] S. E. Potts, G. Dingemans, C. Lachaud, W. M. M. Kessels, Plasma-
512 enhanced and Thermal Atomic Layer Deposition of Al₂O₃ Using
513 Dimethylaluminum Isopropoxide, [Al(CH₃)₂(μ-OⁱPr)]₂, as an Alterna-
514 tive Aluminum Precursor, *Journal of Vacuum Science & Technology A*
515 30 (2012) 021505.
- 516 [35] M. Shirazi, S. D. Elliott, Cooperation Between Adsorbates Accounts
517 for the Activation of Atomic Layer Deposition Reactions, *Nanoscale* 7
518 (2015) 6311–6318.
- 519 [36] R. A. Wind, S. M. George, Quartz Crystal Microbalance Studies of
520 Al₂O₃ Atomic Layer Deposition Using Trimethylaluminum and Water
521 at 125 °C, *The Journal of Physical Chemistry A* 114 (2010) 1281–1289.
522 PMID: 19757806.
- 523 [37] H. H. Sønsteby, A. Yanguas-Gil, J. W. Elam, Consistency and Repro-
524 ducibility in Atomic Layer Deposition, *Journal of Vacuum Science &*
525 *Technology A* 38 (2020) 020804.
- 526 [38] V. Verlaan, L. R. J. G. van den Elzen, G. Dingemans, M. C. M. van de
527 Sanden, W. M. M. Kessels, Composition and Bonding Structure of

- 528 Plasma-assisted ALD Al₂O₃ Films, *physica status solidi c* 7 (2010) 976–
529 979.
- 530 [39] A. Dillon, A. Ott, J. Way, S. George, Surface Chemistry of Al₂O₃
531 Deposition Using Al(CH₃)₃ and H₂O in a Binary Reaction Sequence,
532 *Surface Science* 322 (1995) 230 – 242.
- 533 [40] A. A. Dameron, S. D. Davidson, B. B. Burton, P. F. Carcia, R. S.
534 McLean, S. M. George, Gas Diffusion Barriers on Polymers Using Mul-
535 tilayers Fabricated by Al₂O₃ and Rapid SiO₂ Atomic Layer Deposition,
536 *The Journal of Physical Chemistry C* 112 (2008) 4573–4580.
- 537 [41] A. I. Abdulgatov, Y. Yan, J. R. Cooper, Y. Zhang, Z. M. Gibbs, A. S.
538 Cavanagh, R. G. Yang, Y. C. Lee, S. M. George, Al₂O₃ and TiO₂ Atomic
539 Layer Deposition on Copper for Water Corrosion Resistance, *ACS Ap-
540 plied Materials & Interfaces* 3 (2011) 4593–4601. PMID: 22032254.
- 541 [42] H. Zhang, L. Guo, Q. Wan, Nanogranular Al₂O₃ Proton Conducting
542 Films for Low-voltage Oxide-based Homojunction Thin-film transistors,
543 *Journal of Materials Chemistry C* 1 (2013) 2781–2786.

Highlights

- Concentration and source of impurity H was studied using isotopic labeling
- H and C impurities decrease with increasing deposition temperature and purge time
- Hydrogen isotopes can migrate in the film even at room temperature
- Migration occurs only if H concentration in the film is high enough

Isotopic
exchange



Credit Author Statement

Sami Kinnunen: Investigating, Visualisation, Writing - original draft preparation. **Kai Arstila:** Investigating, Writing – Review & editing. **Timo Sajavaara:** Supervision, Writing – Review & editing

Journal Pre-proofs